

Manuscript Number:

Title: Constraining the transport time of lithogenic sediments to the Okinawa Trough (East China Sea)

Article Type: SI:TengCriticalZone

Keywords: sediment, transport time, comminution age, U-series isotope, Okinawa Trough, East China Sea, Changjiang (Yangtze River)

Corresponding Author: Dr. Shouye Yang, Ph.D.

Corresponding Author's Institution: State Key Laboratory of Marine Geology, Tongji University

First Author: Chao Li, Dr.

Order of Authors: Chao Li, Dr.; Roger Francois, Prof.; Shouye Yang, Ph.D.; Jane Barling, Dr.; Sophie Darfeuil; Yiming Luo, Dr.; Dominique Weis, Prof.

Abstract: The transport time of siliciclastic sediments from their continental sites of formation to their final loci of deposition on the seafloor is an important parameter bearing on our understanding of land-sea interactions, climate variability, and landscape evolution. $^{234}\text{U}/^{238}\text{U}$ activity ratios of the lithogenic fraction from late Quaternary sediment deposited in the Okinawa Trough, East China Sea, were reported in this study. On basis of $^{234}\text{U}/^{238}\text{U}$ activity ratios, comminution ages and transport times were calculated using recoil loss factors (f_{RL}) derived from different equations based on grain size distribution. The transport times were longer (approximately 200 ± 100 kyrs) for the Okinawa Trough sediments deposited between 27-14 ka, decreased gradually between 14-7 ka, and stayed relatively short (<100 kyrs) thereafter. Mineralogical, geochemical and isotopic evidences indicate that changes in sediment transport time correspond well with the shift of sediment provenance predominantly from Asia's interior prior to 14 ka to Taiwan Island after 7 ka. This study offers the first and robust constraint on time scale of sediment transport process in East Asia marginal sea, which is characterized by unique sediment source-to-sink transport pattern. The result illustrates the potential of this approach to decipher climate-related changes in the mode of supply of lithogenic sediment to marginal seas. It also highlights current difficulties in obtaining quantitative estimates of comminution age, mostly because of uncertainties in constraining initial ($^{234}\text{U}/^{238}\text{U}$) of parent rocks and in estimating the recoil loss factor.

1 Constraining the transport time of lithogenic sediments to the
2 Okinawa Trough (East China Sea)

3

4 **Chao Li¹, Roger Francois², Shouye Yang^{1,*}, Jane Barling³, Sophie Darfeuil^{2,4},**
5 **Yiming Luo^{2,5} and Dominique Weis²**

6 *1. State Key Laboratory of Marine Geology, Tongji University, Shanghai 200092, P.*
7 *R. China*

8 *2. Pacific Centre for Isotopic and Geochemical Research, Department of Earth and*
9 *Ocean Sciences, University of British Columbia, Vancouver B.C. V6T 1Z4, Canada*

10 *3. Department of Earth Sciences, University of Oxford, South Parks Road, Oxford*
11 *OX1 3AN, UK*

12 *4. CEREGE, UMR7330, Aix-Marseille University, CNRS, IRD, Collège de France,*
13 *Technopole de l'Arbois BP80, 13545 Aix-en-Provence, France*

14 *5. Department of Oceanography, Dalhousie University, 1355 Oxford Street, Halifax*
15 *N.S. B3H 4J1, Canada.*

16

17 * Corresponding author: Shouye Yang (syyang@tongji.edu.cn)

18

Abstract

The transport time of siliciclastic sediments from their continental sites of formation to their final loci of deposition on the seafloor is an important parameter bearing on our understanding of land-sea interactions, climate variability, and landscape evolution. $^{234}\text{U}/^{238}\text{U}$ activity ratios of the lithogenic fraction from late Quaternary sediment deposited in the Okinawa Trough, East China Sea, were reported in this study. On basis of $^{234}\text{U}/^{238}\text{U}$ activity ratios, comminution ages and transport times were calculated using recoil loss factors (f_α) derived from different equations based on grain size distribution. The transport times were longer (approximately 200 ± 100 kyrs) for the Okinawa Trough sediments deposited between 27–14 ka, decreased gradually between 14–7 ka, and stayed relatively short (<100 kyrs) thereafter. Mineralogical, geochemical and isotopic evidences indicate that changes in sediment transport time correspond well with the shift of sediment provenance predominantly from Asia's interior prior to 14 ka to Taiwan Island after 7 ka. This study offers the first and robust constraint on time scale of sediment transport process in East Asia marginal sea, which is characterized by unique sediment source-to-sink transport pattern. The result illustrates the potential of this approach to decipher climate-related changes in the mode of supply of lithogenic sediment to marginal seas. It also highlights current difficulties in obtaining quantitative estimates of comminution age, mostly because of uncertainties in constraining initial ($^{234}\text{U}/^{238}\text{U}$) of parent rocks and in estimating the recoil loss factor.

Key words: sediment, transport time, comminution age, U-series isotope, Okinawa Trough, East China Sea, Changjiang (Yangtze River)

1. Introduction

The East China Sea (ECS) links the Eurasian continent and the Pacific Ocean, and it is characterized by broad continental shelf and huge terrigenous sediment input from adjacent rivers. The river-dominated marginal sea witnessed the complex sediment source-to-sink transport and sedimentary environmental changes during the late Quaternary (Li et al., 2014). In particular, two distinguishing river systems determine the sediment source-to-sink process in this region, the Changjiang (Yangtze River), one of the largest river in the world, and the small mountainous rivers, especially those in Taiwan Island (Yang et al., 2015). The sediment transferring from both river systems is thus of great significance to the sedimentary records and chemical evolution in the ECS. In view of this, the sediment provenances, depositional processes and paleoenvironmental changes in the ECS have been extensively investigated over the last decade (Dou et al., 2010a, 2015; Li et al., 2015b). However, the absolute time scale of sediment transport in the ECS and East Asia continental margin, which is critical to the sediment source-to-sink processes, remains to be unknown (Li et al., 2015a).

The timescale of lithogenic sediment cycling is crucial for assessing the long-term carbon burial by erosion, determining the factors controlling the flux of lithogenic material to the ocean, and understanding the stratigraphic evolution of continental margins. The lithogenic material accumulating in the Okinawa Trough (OT), was mostly derived from the Changjiang and Taiwan Island (Dou et al., 2010a, b), and has formed continuous and thick sediment strata during the late Quaternary. As one of the major sinks for terrigenous input in the ECS (Qin et al., 1987), the late Quaternary deposition in the OT provides an important archive for investigating the evolution of Changjiang and Taiwan Island river systems in relation to climate change and sea

level rise (Li et al., 2015a).

U-series nuclides are widely used to constrain the rates of earth surface processes (Bourdon et al., 2003; Chabaux et al., 2008, 2011; Dosseto et al., 2008; Ma et al., 2010; Vigier and Bourdon, 2011; Dosseto, 2015), and a new approach has recently been proposed to estimate the “transport time” of lithogenic particles from their comminution ages (i.e. the time that has elapsed since their formation by continental weathering) based on their $^{234}\text{U}/^{238}\text{U}$ activity ratios (DePaolo et al., 2006, 2012; Maher et al., 2006; Dosseto et al., 2010; Lee et al., 2010; Handley et al., 2013a). This comminution dating approach is primarily based on $^{234}\text{U}/^{238}\text{U}$ disequilibrium resulted from recoil loss in fine-grained sediments. The method has been applied in North Atlantic deep sea sediment (DePaolo et al., 2006), paleo-channel sediment (Dosseto et al., 2010; Lee et al., 2010; Handley et al., 2013a, b) and Antarctica ice core (Aciego et al., 2011), which yielded reasonable timescale of sediment transfer across various geology settings. However, its theoretical basis, parameter calculation (e.g. recoil loss factor) and external constraint are still under debate. Therefore, further testing and consideration of the methodology are necessary to improve the accuracy of age estimation and to develop its application in future studies.

The goal of this study is to apply the comminution age method to estimate the transport time of lithogenic sediments deposited in OT and further to compare the results with changes in sediment provenance deduced from geochemical and isotopic analysis (Dou et al., 2010a, b, 2012, 2015). Besides, this study also makes the first attempt of applying the comminution age method in river-dominated marginal sea, which will be an important exploration and contribution to the U-series disequilibrium study.

2. Comminution age theory

The determination of comminution age is based on the continuous loss of ^{234}U from the thin outer layer (~ 30 nm in thickness) of silicate mineral particles, which results from alpha recoil (Kigoshi, 1971). During this process, the ^{234}Th is ejected due to ^{238}U alpha-decay and then ^{234}Th decays to ^{234}U with a half-life of only 24 days. Because ^{234}Th ejection from a mineral grain is only possible from this very thin outer layer, the loss of ^{234}U is a function of the surface area to volume of the particle (Vigier and Bourdon, 2011). The continuous loss of ^{234}U results in a measurable decrease in ($^{234}\text{U}/^{238}\text{U}$) (parentheses denote activity ratios throughout this paper) of the entire grain only when the surface area to volume increases to certain extent (approximately at ~ 50 micron diameter) (DePaolo et al., 2006). Thus, once such small particles have been formed by continental weathering and erosion, their ($^{234}\text{U}/^{238}\text{U}$) ratios start to decrease. If the small particle undergoes no additional abrasion or loss of depleted surface, their ($^{234}\text{U}/^{238}\text{U}$) eventually reaches a steady state value, which is determined by the size and shape of the particles and the roughness of their surface. However, it is notable that preferential loss of ^{234}U relative to ^{238}U may occur via leaching during weathering of the source rock and/or sediment transport process. Although DePaolo et al. (2006) and Maher et al. (2006) have argued that ^{234}U depletion can be determined by a-recoil alone, other studies suggest (or have assumed) that preferential leaching from damaged tracks of mineral lattice is also important (Eyal and Olander, 1990; Bourdon et al., 2009; Andersen et al., 2013). With all these assumption, the “comminution age” (t_{com}) can be calculated from Eq. (1) (DePaolo et al., 2006):

$$t_{\text{com}} = -\frac{1}{\lambda_{234}} \ln \left[\frac{A_{\text{meas}} - (1 - f_{\alpha})}{A_0 - (1 - f_{\alpha})} \right] \quad (1)$$

where A_0 is ($^{234}\text{U}/^{238}\text{U}$) of the parent rock, A_{meas} is ($^{234}\text{U}/^{238}\text{U}$) of the sample studied, λ_{234} is the decay constant of ^{234}U , and f_{α} is the recoil loss factor, i.e. the fraction of ^{238}U decay in the sample that results in the ejection of a ^{234}Th atom (Kigoshi, 1971;

118 Maher et al., 2006). The “transport time” of fine-grained particles between sites of
119 their formation from parent rocks to sites of final deposition (e.g. seafloor) can then
120 be calculated by subtracting the depositional age, obtained from core chronology,
121 from the comminution age. Obviously, calculated “transport times” integrate the
122 storage time of particles in weathering profiles, their transport time in river channels,
123 and residence time in alluvial plains and on the continental shelf (Dosseto et al.,
124 2010).

125 3. Study area

126 The Okinawa Trough (Fig. 1a) is a typical back-arc basin of the Ryukyu trench-
127 arc system, bounded by the Ryukyu Ridge and Trench to the south and east, and by
128 the ECS shelf to the north and west. The entire OT is arcuate, convex toward the west
129 Pacific, from Japan to Taiwan. It has a large section of more than 1,000 m in depth
130 and the deepest part, near Taiwan Island, is about 2,270 m deep. The OT shoals
131 gradually northeastward toward Japan and is underlain by about 1~2 km of sediment
132 (Lee et al., 1980). The OT is a depositional basin with a relatively high rate of
133 sedimentation of primarily terrigenous sediment from the East Asia continent, ESC
134 continental shelf and island arc via the numerous adjacent rivers (Qin et al., 1987). As
135 a passage linking East Asian continent to the west Pacific Ocean, the OT may serve as
136 a sensitive reflection of environmental transition between the ocean and continental
137 settings. The most striking oceanographic feature in the OT is the Kuroshio Current
138 which is the largest western boundary current in the North Pacific Ocean.

139 Among the numerous rivers entering the ESC, the Changjiang is the largest river
140 in East Asian continent. It originates from the Tibet Plateau and its catchment, which
141 is up to 1.8×10^6 km² in area, is primarily situated on the Yangtze Craton. Geologically,

the Changjiang catchment comprises complex rock types including Archean metamorphic rocks, Jurassic sandstone, Paleozoic carbonate and sedimentary rocks, Mesozoic–Cenozoic igneous and clastic rocks, and Quaternary detrital sediments (Yang et al., 2004). Based on the long-term hydraulic observation, the Changjiang annually delivers about 470 Mt suspended sediments to the ECS (Milliman and Farnsworth, 2011). Major part of the Changjiang-derived sediment is trapped in its estuary and deposited on adjacent ECS shelf (Liu et al., 2007), while the remainder may be transported to the Okinawa Trough, resulting in a thick sedimentary deposit (Qin et al., 1987).

Apart from the large rivers, small rivers in East Asia also played an important role in sedimentation in the ECS, in particular the mountainous rivers from Taiwan Island (Kao and Milliman, 2008). The island of Taiwan is characterized by its strong tectonic uplift at a rate of 5–10 mm/yr (Shin and Teng, 2001), and high physical erosion rate up to 3–6 mm/yr (Dadson et al., 2003). Together with the frequent typhoon and earthquake events, the rivers in Taiwan island discharge about 180 Mt/yr sediment to the surrounding marginal seas, showing one of the highest sediment yields in the world (Kao and Milliman, 2008). The Taiwan river basins are mainly composed of sedimentary rocks and epimetamorphic rocks including sandstone, shale, slate and phyllite, with rare occurrence of acidic rocks. The Zhuoshui (also named Chuoshui) River as the largest one in Taiwan Island, is originated from Central Mountain Range, with an elevation of about 3,000 m and the total length of 186 km.

4. Samples and Methods

4.1 Sources of river and marine sediment samples

In this study, a total of 24 sediment samples were selected from piston core

DGKS9604 (28°16.64' N, 127°01.43' E, 766 m water depth) taken from the OT in 1996 during the joint Chinese–French DONGHAI Cruise (Fig. 1a). The age model is derived from oxygen isotopic composition and radiocarbon dates measured on planktonic foraminifera *Globigerinoides sacculifer* determined by accelerator mass spectrometry (Yu et al., 2009).

For constraining the sediment transport times of the modern Changjiang River, two sediment samples were collected near Chongqing (CQ) and Nantong (NT), which represent the upstream and estuary (Fig. 1c), respectively. Another two samples from Taiwan Island were collected in the Zhuoshui River from the upstream (ZS-1) and estuary (ZS-2) (Fig. 1d), respectively. Detailed sample information is shown in Table 1.

4.2 $^{234}\text{U}/^{238}\text{U}$ measurements

The river and marine sediment samples were leached with 1.5N HCl for 30 minutes at room temperature to remove carbonate and authigenic phases, following the method by DePaolo et al. (2006). After centrifugation, about 0.1 g of the residue was used for grain size analysis, and 0.2 g was dried and ground for the measurement of uranium isotopes. The powdered samples were digested in mixed acids (HClO_4 -HF- HNO_3), before U separation on UTEVA[®] resin (98% column recovery for U; chemistry blank 0.89 ng U corresponding to ca. 0.3% of the samples). The measurement of ($^{234}\text{U}/^{238}\text{U}$) ratios was carried out on a Multi-Collector ICP-MS (Nu 021; Nu Instruments Ltd., UK) at the Pacific Centre for Isotopic and Geochemical Research, University of British Columbia, following the procedure described in Andersen et al. (2004). We used standard bracketing with CRM-145B in which ($^{234}\text{U}/^{238}\text{U}$) was verified against Plešovice zircons (Sláma et al., 2008). The $\delta^{234}\text{U}$ value obtained for CRM-145B relative to these zircons ($-37.47 \pm 1.24\text{‰}$ (2 standard

deviations, n=5)) was within the error of $\delta^{234}\text{U}$ reported for CRM-145B ($-36.50 \pm 0.14\%$ (Andersen et al., 2004)). The latter value was thus used as reference for the calculation of activity ratios in the samples. The external reproducibility of the measurements was estimated by analyzing BCR-2 ($\delta^{234}\text{U} = 4.13 \pm 2.29\%$ (2 standard deviations, n=54)).

4.3 Determination of grain size distributions

The grain size distribution of the sediment samples was measured on a Malvern Mastersizer 3000 particle size analyzer at the University of British Columbia, while grain size distribution of the river samples was measured on a Beckman Coulter LS230 particle size analyzer at the State Key Laboratory of Marine Geology, Tongji University.

5. Calculation of comminution ages and transport time from ($^{234}\text{U}/^{238}\text{U}$)

The accuracy of comminution ages calculated with Eq. (1) depends on the validity of the assumptions made regarding A_o and f_a . One assumption is that in the absence of large crustal fluid flow, the U-series decay chain of continental rocks is generally in secular equilibrium (Vigier and Bourdon, 2011). Supporting this view, a systematic investigation of ($^{234}\text{U}/^{238}\text{U}$) in rocks taken from a glacial outwash yielded values very close to secular equilibrium (1.00 ± 0.01), independent of lithology (DePaolo et al., 2012). However, Handley et al. (2013b) found significant ^{234}U depletion in sedimentary rocks samples, raising the possibility that the assumption of secular equilibrium in parent rocks may not always be correct. While A_o could potentially be estimated when the source rock of sediment can be clearly identified, in most instances this is very difficult and thus A_o is often assumed to be 1 (DePaolo et al., 2006, 2012; Maher et al., 2006; Dosseto et al., 2010; Lee et al., 2010; Handley et al.,

2013a). Determining A_o for the lithogenic sediments from the Changjiang River, ECS shelf and OT as well is particularly difficult considering the very complicated and diverse provenance rock types in the large Changjiang drainage basin, and complex sediment source-to-sink transport in the continental margin.

The recoil loss factor (f_α) is also difficult to accurately estimate because it depends on the shape and surface roughness of mineral grains. Different approaches have been proposed to estimate f_α based on (a) the distribution of grain size in the sample for U isotope analysis, and the assumptions for changes in surface roughness and grain aspect ratio as a function of grain size (DePaolo et al., 2006; Maher et al., 2006; Dosseto et al., 2010; Lee et al., 2010; Handley et al., 2013a); (b) surface area measurements (e.g., Brunauer-Emmett-Teller (BET)) with fractal correction to account for the significant size difference between the adsorbed gas molecules used for surface area measurement and the recoil length scale of alpha particles (Olley et al., 1997; Aciego et al., 2011; Handley et al., 2013a); (c) ($^{234}\text{U}/^{238}\text{U}$) measured in samples approaching a steady state (i.e. older than 500 ka) (Lee et al., 2010).

In the present study, we estimate f_α using two independent methods based on grain size distribution. The method proposed by DePaolo et al. (2006) is based on Eq. (2):

$$f_\alpha = \sum_{r=L/2}^{r_{max}} X(r)\beta(r)\lambda_s(r)\frac{3}{4}\left(\frac{L}{r} - \frac{L^3}{12r^3}\right)\Delta r \quad (2)$$

Where $X(r)$ is the volume fraction of different particle size intervals (Δr) present in the sample analyzed for U isotopic ratio, $\beta(r)$ is their aspect ratio, $\lambda_s(r)$ is their surface roughness factor, and L is the α -recoil length generally taken to be 30 nm. Following previous studies (DePaolo et al., 2006; Dosseto et al., 2010; Handley et al., 2013a), we also assume that: (a) the aspect ratio ($\beta(r)$) of particles with $r < 25 \mu\text{m}$ increases

linearly with decreasing grain size, from 1 for the largest grains to 10 for the smallest;
and (b) the surface roughness $\lambda_s(r)$ increases linearly with grain size from 1 for the
smaller grains to 2 (DePaolo et al., 2006) or 17 (Handley et al., 2013a) for the larger
grain size. Thereby, a range of comminution age for each of our samples can be
obtained on the basis of the above assumptions.

Another approach to evaluate f_α assumes a constant surface roughness (λ_s) and a
constant dimensionless grain shape factor K (Cartwright, 1962) over the entire grain
size spectrum (Lee et al., 2010):

$$f_\alpha = \sum_L^{d_{max}} X(d) \frac{LK}{4d} \lambda_s \Delta d \quad (3)$$

Where d is the grain diameter and L is the recoil distance. Freshly crushed silicate
minerals generally have a relatively constant $\lambda_s = 7$ over a wide range of grain size
(White and Peterson, 1990) and this value was used for Eq. (3). $K = 6$ is the grain
shape factor for spheres, but for silicate minerals with mean particle sizes ranging
from 0.2 to 10 μm , $K = 14\text{--}18$ (Cartwright, 1962). We thus calculated f_α with Eq. (3)
using a constant $\lambda_s = 7$ and $K = 6$ or 18 to obtain a range of comminution ages and
transport times for our samples.

Notwithstanding the uncertainties raised by the basic premises of the approach,
we calculate the transport times of the lithogenic sediments deposited in the OT from
their ($^{234}\text{U}/^{238}\text{U}$), assuming that $A_o = 1$, and estimate f_α using the two approaches
described above. The goal of this study is to investigate whether there are coherent
changes in the calculated transport times of lithogenic particles, and whether the
transport times are consistent with changes in sediment provenance reconstructed in
earlier studies (Dou et al., 2010a, b).

6. Results

6.1 Uranium isotopic ratios

The ($^{234}\text{U}/^{238}\text{U}$) ratios of the OT sediment range from 0.917 to 1.040, with a clear temporal trend (Fig. 2a). The ratios are relatively low and uniform between 27 and 14 ka with a mean value of 0.924, increase gradually between 14 and 7 ka, and stay high and closer to secular equilibrium after 7 ka. Some samples from the upper section of the core have ($^{234}\text{U}/^{238}\text{U}$) values >1 , which cannot be directly interpreted in terms of comminution ages.

The ($^{234}\text{U}/^{238}\text{U}$) ratios of the Changjiang River sediments range from 0.979 ± 0.002 at CQ to 0.941 ± 0.001 at NT, while the ($^{234}\text{U}/^{238}\text{U}$) ratios for the Zhuoshui River sediments ranges from 1.002 ± 0.002 at ZS-1 to 0.960 ± 0.001 at ZS-2 (Table 1). Both rivers show decreasing ($^{234}\text{U}/^{238}\text{U}$) ratios towards the lower reaches.

6.2 Sediment grain size and f_α

The sediment samples from the OT are dominated by silt ($60 \pm 7\%$) and clay ($37 \pm 5\%$), with low sand content ($2 \pm 2\%$), and downcore variations of mean grain size is small (Table 1; Fig. 3a,b). Similarly, f_α yields small changes with core depth although the absolute values of f_α estimated by different assumptions vary significantly (Table 2; Fig. 3c).

The river particles from the Changjiang have similar proportions of silt (59%) and clay (41%) as the OT sediments, without sand-size material, while the samples collected from the Zhuoshui River consist of more silt (74-80%) and less clay (19-25%) (Table 1). f_α estimates for the Changjiang river particles are higher, while those for the Zhuoshui river particles are slightly lower compared to the OT sediments.

6.3 Calculated transport times

Transport times of the river and marine sediments derived from f_{α} with two different methods (Eq. (2) and (3)) are listed in Table 2. The estimated transport times for the OT sediment are longer during the last glacial period and gradually decrease through the last deglaciation, mirroring the downcore variability of ($^{234}\text{U}/^{238}\text{U}$). The range of transport time obtained with Eq. (3) for K of 6 ~18 is overall larger than that obtained with Eq. (2) for λ_{max} of 2~17 (Fig. 4a).

The estimated transport times for the suspended particles collected in the Changjiang and Zhuoshui rivers increase downstream. Particles from the upper Changjiang (CQ) yield a transport time of 21–67 ka, compared to 66–253 ka for particles from the lower Changjiang (NT). Likewise, the transport time for suspended particles from the upper Zhuoshui (ZS-1) is near zero, while the lower Zhuoshui (ZS-2) sample yields transport times of 82–344 kyrs showing larger range than the counterpart of the Changjiang (Table 2).

7. Discussions

7.1 Uncertainties of comminution age calculation in the OT sediment

7.1.1 ($^{234}\text{U}/^{238}\text{U}$) in marine sediments

It is notable that some OT sediments show ($^{234}\text{U}/^{238}\text{U}$)>1, which thus yield negative comminution age. These abnormal ($^{234}\text{U}/^{238}\text{U}$) values are probably a result of the non-conservative behavior of uranium in seawater. Uranium with ($^{234}\text{U}/^{238}\text{U}$) close to that of seawater (1.14) is expected to be present in the biogenic (carbonates) and authigenic (oxides, sulfides and clays) phases of marine sediment. An appropriate chemical leaching method to remove authigenic and biogenic phases is thus critical to obtain accurate comminution age. The leaching method must leave intact the 30 nm outer layer of the lithogenic particles, which actually carries the alpha-recoil signal

(DePaolo et al., 2012). Despite some attempts, developing an optimal leaching procedure is still working in progress (Maher et al., 2006; Dosseto et al., 2010; Lee et al., 2010; Suresh et al., 2014; Martin et al., 2015). In our study, a simple acid leaching (1.5N HCl, 30 minutes at room temperature) provided by DePaolo et al. (2006) is employed which is applicative for north Atlantic marine sediment.

The carbonate content in the core DGKS9604 sediment is overall low (5–10%) prior to 14 ka, and gradually increases to 20–25% after 7 ka (Fig. 2b). The uranium content of biogenic calcite is low, about 20–30 ppb (Russell et al., 1994). Since biogenic calcite readily dissolves in 1.5N HCl, this small pool of uranium should have been effectively removed by our pre-treatment.

The main mechanism whereby authigenic U is added to marine sediment is by reduction of soluble U(VI) to insoluble U(IV) in suboxic pore water (Klinkhammer and Palmer, 1991), which results in a gradual increase in sediment U concentration with burial depth. The organic carbon content in the core sediments ranges between 1.0% and 1.5%, without a clear trend with depth (Fig. 2c). In contrast, the total sulfur content, which mostly reflects the formation of sulfide minerals as a result of sulfate reduction, increases with depth (Fig. 2d). This observation suggests that reducing conditions in the deeper section of the core could have resulted in the accumulation of authigenic U. Most authigenic sulfide minerals would be dissolved during the acid pre-treatment, except pyrite which is common in the ECS shelf and OT (Qin, 1994). However, the U/Al₂O₃ ratios (ppm/%; Fig. 2e) in the core sediments decrease towards the lower part of this core, and remain below the ratio reported for the upper continental crust (0.18 ppm/%; (Taylor and McLennan, 1995)). Thus, the level of authigenic U in OT sediment appears to be very low, which is expected considering very high sedimentation rate of lithogenic material at the study site, about 29 cm/ky

(Dou et al., 2010a).

Secondary clay minerals could also have high ($^{234}\text{U}/^{238}\text{U}$) ratios relative to their amalgamated pellet grain size, and if present in abundance, could offset calculations based on grain size (Handley et al., 2013a). However, although the core sediments contain about 40% clays, Dou et al. (2010b) showed that these clays are primarily lithogenic with major sources from the surrounding land.

In addition, Fe and Mn concentrations are higher towards the sediment-water surface (Fig. 2f). Given that the sediment provenance did not change greatly during the last 7 kyr (Dou et al., 2010a, b), this increase likely reflects the presence of oxides produced by remobilization of Fe and Mn (Froelich et al., 1979). Adsorption of U from bottom water or pore water on these Fe-Mn oxides could contribute authigenic U to the sediments. However, a significant addition of authigenic U by this mechanism is not supported by the downcore variability of $\text{U}/\text{Al}_2\text{O}_3$, which does not increase concomitantly with $\text{MnO}/\text{Al}_2\text{O}_3$ and $\text{Fe}_2\text{O}_3/\text{Al}_2\text{O}_3$ in the core (Fig. 2f).

In summary, the concentration of authigenic U appears too low to significantly affect the ($^{234}\text{U}/^{238}\text{U}$) of the OT sediment, largely because the much larger addition of lithogenic uranium overwhelms the much slower accumulation rate of authigenic uranium. However, three of the Holocene sediment samples yield ($^{238}\text{U}/^{234}\text{U}$) significantly higher than 1 (Fig. 2a), which suggests significant contribution from authigenic phases, in contradiction with their geochemical composition, and adds ambiguity to the interpretation of these results.

7.1.2 ($^{234}\text{U}/^{238}\text{U}$) of parent rocks— A_0

The initial ($^{234}\text{U}/^{238}\text{U}$) of parent rocks (A_0) is crucial for comminution age calculation. The assumption that $A_0 = 1$ has been widely adopted in earlier studies (DePaolo et al., 2006, 2012; Maher et al., 2006; Dosseto et al., 2010; Lee et al., 2010;

Handley et al., 2013a). Regardless Handley et al. (2013b) has shown that sedimentary rocks may not always be in secular equilibrium, Vigier and Bourdon (2011) summarized that the assumption of initial secular equilibrium for bulk rocks is overall valid although there are small deviations from secular equilibrium for a number of studies.

The Changjiang River drains the typical topography of China continent, with three-grade relief terraces spanning 3500–5000 m, 500–2000 m and less than 500 m in elevation (Fig. 1c). Complex source rocks show large basinal variations within the large catchment. The large size, complex topography and diverse lithology of the drainage basin prevent us from examining A_0 of every type of source rock. Nevertheless, we cannot rule out the possibility that we have overestimated the transport time for the lithogenic sediment by overestimating A_0 .

Taiwan Island has a steep topography and is subjected to a rapid tectonic uplift, resulting in high erosion rates of up to 3–6 mm/yr (Dadson et al., 2003). As a result, the small mountainous rivers in Taiwan show by far the highest sediment yield in the world (Kao and Milliman, 2008). The ($^{234}\text{U}/^{238}\text{U}$) for sediment from the upper Zhuoshui is 1.002 ± 0.002 , revealing that the sediment is quite fresh and still in the state of secular equilibrium.

7.1.3 Recoil loss factor (f_α) and calculated transport time

The three-fold range in f_α calculated with Eq. (2) and (3) (Fig. 3c) suggests that without a better means of constraining this important parameter, estimation of comminution ages will remain a large uncertainty. Considering the variations of f_α between the last glaciation and Holocene from core DGKS9604, however, these estimates still provide useful information. Notwithstanding the large uncertainties in absolute comminution ages, they do indicate a clear change from longer transport

times during the last glacial period to much shorter transport times through the last deglaciation and Holocene (Fig. 4a; Table 2). This is in large part because of the relatively constant grain size (and presumably f_{α}) with depth at our study site, and the sharp contrast in the origins and transport pathways of lithogenic sediments deposited in OT over the last glacial/interglacial climatic cycle.

The transport times calculated with Eq. (2) and (3) overlap but the range is significantly smaller for Eq. (2) (Fig. 4a). The largest and smallest grain shape factors (K) used in Eq. (3) thus appear inconsistent with a reasonable range of parameters for Eq. (2). This may be because the grain size distribution of OT sediment is relatively consistent and thus, the grain shape factors (K) vary only in a small range. Furthermore, $K=6$ for sphere shape grain yields the largest deviation for the calculated transport time, suggesting that the sphere grain model is not applicable for the OT sediment.

Overall, the calculation result suggests that the range of transport times for glacial lithogenic sediments estimated by Eq. (2) (approximately 200 ± 100 kyrs) may provide our best estimates. On the other hand, while clearly shorter (< 100 kyrs), the transport time of lithogenic particles accumulated in the Holocene section is too short to be quantified by the method as presently developed.

7.2 Transport time variations induced by changes of sediment provenance

7.2.1 Provenance changes of the OT sediment since 27 ka based on previous studies

The changes of sediment provenances and paleoenvironment in the OT have been extensively investigated over the last decade (Yang et al., 2015). Generally, the sediment provenances changed gradually in the OT during the last 27 kys. The OT sediment deposited in the last glacial period was mainly derived from East Asian continent and/or the ECS continual shelf through the Changjiang River transport,

while the Taiwan Island became the main sediment source of the OT with the strengthening of Kuroshio Current during the Holocene. This conclusion has been verified by various lines of evidence from rare earth elements (Dou et al., 2010a), Sr (Fig. 4b) and Nd isotopes (Dou et al., 2012; Li et al., 2015b), and clay mineralogy (Diekmann et al., 2008; Dou et al., 2010b; Wang et al., 2015). During the last glacial maximum, the sea level was about 120–135 m lower than today in East Asia marginal sea and the continental shelf was largely exposed (Fig. 1b; Fig. 4c and 4d). The paleo-Changjiang discharged vast fine-grained sediments from the East Asia continent into the mid-outer ECS shelf, and finally to the OT (Yang et al., 2015). At the same time, the main stream of the Kuroshio Current might have diverted eastward (Ujiie et al., 1991) (Fig. 1b), limiting the supply of sediment originating from Taiwan Island. During the period of deglaciation and early Holocene (ca. 14–7 ka), the ECS coastline and paleo-Changjiang river mouth retreated gradually with the continuously rising sea level (Figs 1a and 4d), while the major Kuroshio Current shifted westward over the OT (Ichikawa and Beardsley, 2002). Consequently, the sediment contribution from the Changjiang gradually declined because of increased trapping of the river sediment in the estuary and on the inner shelf, while the sediment supply from Taiwan Island gradually increased with the strengthening of the Kuroshio Current.

7.2.2 Provenance changes of the OT sediments evidenced by ($^{234}\text{U}/^{238}\text{U}$) and transport time

The change of sediment provenance in the OT is consistent with the gradual increase of ($^{234}\text{U}/^{238}\text{U}$) in the core sediments (Fig. 2a). Regardless of possible effect of preferential release of ^{234}U into solution during alteration/dissolution, when a small mineral grain is produced by erosion, it begins to leak ^{234}Th to its surroundings as a result of α -recoil (Bourdon et al., 2003), and the ($^{234}\text{U}/^{238}\text{U}$) starts to decrease. Thus,

value of ($^{234}\text{U}/^{238}\text{U}$) in sediment provides a qualitative measurement of the time since the small grain was produced, which has been coined by DePaolo et al. (2006) as “comminution age”. In our case, the ($^{234}\text{U}/^{238}\text{U}$) ratios are relatively low and uniform (0.924 on average) between 27 and 14 ka, suggesting a longer sediment transport process. In comparison, the ($^{234}\text{U}/^{238}\text{U}$) ratios increase gradually between 14 and 7 ka, and stay high and closer to secular equilibrium after 7 ka, which indicates short sediment transport times. The ($^{234}\text{U}/^{238}\text{U}$) ratios in the core DGKS9604 sediments correspond well with the changes of sediment provenance independently reconstructed by the clay mineralogical, geochemical and Sr-Nd isotopic data.

The ($^{234}\text{U}/^{238}\text{U}$) for the modern Changjiang is 0.979 in the upstream (CQ) and 0.941 in estuarine samples (NT), while the ($^{234}\text{U}/^{238}\text{U}$) from the Zhuoshui River are 1.002 and 0.960 for upper and lower reaches, respectively. The higher ($^{234}\text{U}/^{238}\text{U}$) for the upstream Changjiang sediment (CQ) is probably because of the upper Changjiang basin being featured by active tectonics, high relief and steep river channel (Fig. 1c), which results in fast erosion and rapid transport of small particles after their formation. In contrast, the relatively lower ($^{234}\text{U}/^{238}\text{U}$) ratio in the Changjiang estuary (NT) indicates a longer transport time from the upper valley to the estuary. The lower Changjiang reaches is characterized by well-developed flood plains and numerous lakes in the mid-lower valley (Fig. 1c), which may effectively trap the particles derived from the upper reaches, and thereby increase their residence times in the mid-lower Changjiang basin. In comparison, the ($^{234}\text{U}/^{238}\text{U}$) ratio in the Zhuoshui river sediments are over larger than in the Changjiang samples, suggesting short comminution ages in Taiwan Island. Taiwan Island has a rugged topography and high denudation rates (Dadson et al., 2003). Short river courses, steep relief and high monsoon rainfalls account for the fast sediment transfer from Taiwan Island to the sea

(Kao and Milliman, 2008).

The ($^{234}\text{U}/^{238}\text{U}$) variation in the OT sediments, which represents the qualitative constraint on time scale of sediment transport based on comminution age theory, provides independent and robust evidence to verify the change of sediment source from East Asia continent and/or ECS shelf in the last glaciation to Taiwan Island during the Holocene. The time scale of sediment source-to-sink transport process can be quantitative achieved with a reliable estimation of the fraction of ^{234}Th ejected due to α -recoil (i.e. f_α).

This study indicates that the transport times average approximately at 200 ± 100 kyrs for the glacial lithogenic sediments in the OT, and < 100 kyrs for the Holocene sediments. The calculated sediment transport times mirror the variations of ($^{234}\text{U}/^{238}\text{U}$) in the core sediments. The transport time for the Changjiang estuary sediment is 120 ± 30 kyrs or 160 ± 90 kyrs based on two different approaches, which is roughly comparable to the transport times for the last glacial sediments in the OT. Their difference in transport time could reflect the transit time of lithogenic particles from the paleo-Changjiang catchment to ECS shelf and finally to OT. Alternatively, the addition of sediments reworked from the exposed shelf (i.e. sediments that were deposited on the shelf during earlier high sea level stands) could also contribute sediment to the OT, which might have increased the sediment transport time defined by ($^{234}\text{U}/^{238}\text{U}$) in this study. Yet, the transport time for Zhuoshui estuary sediment is overlong, which is 146 ± 60 kyrs or up to 210 ± 130 kyrs derived from different calculations. Obviously, the calculation of sediment transport time in Zhuoshui estuary shows extremely large range, which probably bears significant uncertainties due to f_α calculation. Notwithstanding, the ($^{234}\text{U}/^{238}\text{U}$) of Zhuoshui estuarine sediment provide a more convinced constraint on time scale of sediment transport in Zhuoshui

River.

8. Conclusion

In this study, we estimate the sediment transport times in the central Okinawa Trough based on the comminution age theory. The core DGKS9604 sediments with a depositional age of about 27 ka were recovered for the measurement of ($^{234}\text{U}/^{238}\text{U}$) ratios and calculation of sediment transport time. The ($^{234}\text{U}/^{238}\text{U}$) ratios for the core sediments show a clear temporal trend, which is relatively low and uniform between 27 and 14 ka, while stay high and closer to secular equilibrium after 7 ka. The variations of ($^{234}\text{U}/^{238}\text{U}$) in the OT provide qualitative constraints on the time scale and thus the pathways of sediment transport from land to sea, which correspond well with the changes of sediment provenance reconstructed by independent evidences of clay mineralogy, geochemical and Sr-Nd isotopic data. The calculated transport time for the OT sediments is longer (approximately 200 ± 100 kyrs) between 27–14 ka, but relatively short (<100 kyrs) after 7 ka. The longer transport time before 14 ka implies that the detrital sediments was predominantly derived from East Asian continent and/or the ECS shelf, while the shorter transport time after 7 ka suggesting the sediment source from Taiwan Island.

Our study confirms that the comminution age estimates based on ($^{234}\text{U}/^{238}\text{U}$) can provide deep insight into the source-to-sink transport of lithogenic sediments from land to ocean margins. However, they also highlight the current limitations of this method and the need for more precisely estimating the recoil loss factor (f_α) and ($^{234}\text{U}/^{238}\text{U}$) of parent rocks (A_0), in order to obtain more robust and quantitative results. Nonetheless, the relatively constant grain size and geochemically-constrained changes in sediment provenance of the OT facilitate the calculation and interpretation of comminution ages in this unique river-dominated marginal setting. Regardless the

large uncertainties in sediment transport time calculation, this study offers the first constraint on the time scale of sediment source-to-sink transport process in East Asia continental margin, which may greatly improve our understanding on the late-Quaternary land-sea interaction, and is also an important supplementary to U-series disequilibrium community.

Acknowledgements

This work was supported by research funds awarded by the National Natural Science Foundation of China (Grant Nos. 41306040, 41225020 and 41376049). Roger Francois acknowledges financial support from the Natural Sciences and Engineering Research Council of Canada. Chao Li acknowledges financial support from China Postdoctoral Science Foundation (2015M570384). We thank Yanguang Dou for providing some reference data, Zhenxia Liu and Hua Yu for providing core samples, and Maureen Soon for assistance in data acquisition. Discussions with Anthony Dosseto greatly inspire this work and improve the quality of this manuscript.

References:

- Aciego, S., Bourdon, B., Schwander, J., Baur, H., Forieri, A., 2011. Toward a radiometric ice clock: uranium ages of the Dome C ice core. *Quaternary Science Reviews*, 30(19-20): 2389-2397.
- Andersen, M., Stirling, C., Potter, E.-K., Halliday, A., 2004. Toward epsilon levels of measurement precision on $^{234}\text{U}/^{238}\text{U}$ by using MC-ICPMS. *International Journal of Mass Spectrometry*, 237(2): 107-118.
- Andersen, M.B., Vance, D., Keech, A.R., Rickli, J., Hudson, G., 2013. Estimating U

532 fluxes in a high-latitude, boreal post-glacial setting using U-series isotopes in soils
533 and rivers. *Chemical Geology*, 354: 22-32.

534 Bourdon, B., Bureau, S., Andersen, M.B., Pili, E., Hubert, A., 2009. Weathering rates
535 from top to bottom in a carbonate environment. *Chemical Geology*, 258(3-4): 275-
536 287.

537 Bourdon, B., Turner, S., Henderson, G.M., Lundstrom, C.C. (Eds.), 2003. Introduction
538 to U-series geochemistry. *Reviews in mineralogy and geochemistry*, 52.
539 Geochemical Society-Mineralogical Society of America, Washington, DC, 1-21
540 pp.

541 Cartwright, J., 1962. Particle shape factors. *Annals of Occupational Hygiene*, 5(3):
542 163-171.

543 Chabaux, F., Bourdon, B., Riotte, J., 2008. U-series geochemistry in weathering
544 profiles, river waters and lakes. *Radioactivity in the Environment*, 13: 49-104.

545 Chabaux, F., Ma, L., Stille, P., Pelt, E., Granet, M., Lemarchand, D., di Chiara
546 Roupert, R., Brantley, S.L., 2011. Determination of chemical weathering rates
547 from U series nuclides in soils and weathering profiles: Principles, applications
548 and limitations. *Applied Geochemistry*, 26: S20-S23.

549 Dadson, S.J., Hovius, N., Chen, H., Dade, W.B., Hsieh, M.L., Willett, S.D., Hu, J.C.,
550 Horng, M.J., Chen, M.C., Stark, C.P., 2003. Links between erosion, runoff
551 variability and seismicity in the Taiwan orogen. *Nature*, 426(6967): 648-651.

552 DePaolo, D.J., Lee, V.E., Christensen, J.N., Maher, K., 2012. Uranium comminution
553 ages: Sediment transport and deposition time scales. *Comptes Rendus Geoscience*,
554 344(11-12): 678-687.

555 DePaolo, D.J., Maher, K., Christensen, J.N., McManus, J., 2006. Sediment transport
556 time measured with U-series isotopes: Results from ODP North Atlantic drift site

557 984. *Earth and Planetary Science Letters*, 248(1-2): 394-410.

558 Diekmann, B., Hofmann, J., Henrich, R., Fütterer, D.K., Röhl, U., Wei, K.-Y., 2008.

559 Detrital sediment supply in the southern Okinawa Trough and its relation to sea-

560 level and Kuroshio dynamics during the late Quaternary. *Marine Geology*, 255(1):

561 83-95.

562 Dosseto, A., 2015. *Chemical Weathering (U-Series)*. In: Rink, W.J., Thompson, J.

563 (Editors), *Encyclopedia of Scientific Dating Methods*. Springer Netherlands, pp.

564 152-169.

565 Dosseto, A., Bourdon, B., Turner, S.P., 2008. Uranium-series isotopes in river

566 materials: insights into the timescales of erosion and sediment transport. *Earth and*

567 *Planetary Science Letters*, 265(1-2): 1-17.

568 Dosseto, A., Hesse, P., Maher, K., Fryirs, K., Turner, S., 2010. Climatic and vegetation

569 control on sediment dynamics during the last glacial cycle. *Geology*, 38(5): 395-

570 398.

571 Dou, Y., Yang, S., Li, C., Shi, X., Liu, J., Bi, L., 2015. Deepwater redox changes in the

572 southern Okinawa Trough since the last glacial maximum. *Progress in*

573 *Oceanography*, 135: 77-90.

574 Dou, Y., Yang, S., Liu, Z., Clift, P.D., Shi, X., Yu, H., Berne, S., 2010a. Provenance

575 discrimination of siliciclastic sediments in the middle Okinawa Trough since 30ka:

576 Constraints from rare earth element compositions. *Marine Geology*, 275(1): 212-

577 220.

578 Dou, Y., Yang, S., Liu, Z., Clift, P.D., Yu, H., Berne, S., Shi, X., 2010b. Clay mineral

579 evolution in the central Okinawa Trough since 28ka: Implications for sediment

580 provenance and paleoenvironmental change. *Palaeogeography, Palaeoclimatology,*

581 *Palaeoecology*, 288(1-4): 108-117.

582 Dou, Y., Yang, S., Liu, Z., Li, J., Shi, X., Yu, H., Berne, S., 2012. Sr–Nd isotopic
 583 constraints on terrigenous sediment provenances and Kuroshio Current variability
 584 in the Okinawa Trough during the late Quaternary. *Palaeogeography,*
 585 *Palaeoclimatology, Palaeoecology*, 356-366: 38-47.

586 Dou, Y.G., 2010. Source to sink processes and paleoenvironmental response of
 587 terrigenous sediments in the middle and south Okinawa Trough since 28 ka, PhD
 588 thesis, School of Earth and Ocean Science, Tongji University, Shanghai.

589 Eyal, Y., Olander, D.R., 1990. Leaching of uranium and thorium from monazite: I.
 590 Initial leaching. *Geochimica et Cosmochimica Acta*, 54(7): 1867-1877.

591 Froelich, P.N., Klinkhammer, G.P., Bender, M.L., Luedtke, N.A., Heath, G.R., Cullen,
 592 D., Dauphin, P., Hammond, D., Hartman, B., Maynard, V., 1979. Early oxidation
 593 of organic matter in pelagic sediments of the eastern equatorial Atlantic: suboxic
 594 diagenesis. *Geochimica et Cosmochimica Acta*, 43(7): 1075-1090.

595 Handley, H., Turner, S., Afonso, J.C., Dosseto, A., Cohen, T., 2013a. Sediment
 596 residence times constrained by uranium-series isotopes: a critical appraisal of the
 597 comminution approach. *Geochimica Et Cosmochimica Acta*, 103: 245–262.

598 Handley, H.K., Turner, S.P., Dosseto, A., Haberlah, D., Afonso, J.C., 2013b.
 599 Considerations for U-series dating of sediments: Insights from the Flinders
 600 Ranges, South Australia. *Chemical Geology*, 340: 40-48.

601 Ichikawa, H., Beardsley, R.C., 2002. The current system in the Yellow and East China
 602 Seas. *Journal of Oceanography*, 58(1): 77-92.

603 Kao, S., Milliman, J., 2008. Water and sediment discharge from small mountainous
 604 rivers, Taiwan: The roles of lithology, episodic events, and human activities. *The*
 605 *Journal of Geology*, 116(5): 431-448.

606 Kigoshi, K., 1971. Alpha-recoil thorium-234: dissolution into water and the Uranium-

607 234/Uranium-238 disequilibrium in nature. *Science*, 173(3991): 47-49.
 608 Klinkhammer, G.P., Palmer, M.R., 1991. Uranium in the oceans: Where it goes and
 609 why. *Geochimica et Cosmochimica Acta*, 55(7): 1799-1806.
 610 Lambeck, K., Yokoyama, Y., Purcell, T., 2002. Into and out of the Last Glacial
 611 Maximum: sea-level change during Oxygen Isotope Stages 3 and 2. *Quaternary*
 612 *Science Reviews*, 21(1): 343-360.
 613 Lee, C.-S., Shor, G.G., Bibee, L., Lu, R.S., Hilde, T.W., 1980. Okinawa Trough: origin
 614 of a back-arc basin. *Marine Geology*, 35(1): 219-241.
 615 Lee, V.E., DePaolo, D.J., Christensen, J.N., 2010. Uranium-series comminution ages
 616 of continental sediments: Case study of a Pleistocene alluvial fan. *Earth and*
 617 *Planetary Science Letters*, 296(3-4): 244-254.
 618 Li, C., Yang, S., Lian, E., Bi, L., Zhang, Z., 2015a. A review of comminution age
 619 method and its potential application in the East China Sea to constrain the time
 620 scale of sediment source-to-sink process. *Journal of Ocean University of China*,
 621 14(3): 399-406.
 622 Li, G., Li, P., Liu, Y., Qiao, L., Ma, Y., Xu, J., Yang, Z., 2014. Sedimentary system
 623 response to the global sea level change in the East China Seas since the last glacial
 624 maximum. *Earth-Science Reviews*, 139: 390-405.
 625 Li, T., Xu, Z., Lim, D., Chang, F., Wan, S., Jung, H., Choi, J., 2015b. Sr–Nd isotopic
 626 constraints on detrital sediment provenance and paleoenvironmental change in the
 627 northern Okinawa Trough during the late Quaternary. *Palaeogeography,*
 628 *Palaeoclimatology, Palaeoecology*, 430: 74-84.
 629 Liu, J., Xu, K., Li, A., Milliman, J., Velozzi, D., Xiao, S., Yang, Z., 2007. Flux and
 630 fate of Yangtze River sediment delivered to the East China Sea. *Geomorphology*,
 631 85(3-4): 208-224.

632 Ma, L., Chabaux, F., Pelt, E., Blaes, E., Jin, L., Brantley, S., 2010. Regolith
633 production rates calculated with uranium-series isotopes at Susquehanna/Shale
634 Hills Critical Zone Observatory. *Earth and Planetary Science Letters*, 297(1): 211-
635 225.

636 Maher, K., DePaolo, D.J., Christensen, J.N., 2006. U-Sr isotopic speedometer: Fluid
637 flow and chemical weathering rates in aquifers. *Geochimica Et Cosmochimica*
638 *Acta*, 70(17): 4417-4435.

639 Martin, A.N., Dosseto, A., Kinsley, L.P., 2015. Evaluating the removal of non-detrital
640 matter from soils and sediment using uranium isotopes. *Chemical Geology*, 396:
641 124-133.

642 Milliman, J.D., Farnsworth, K.L., 2011. River discharge to the coastal ocean: a global
643 synthesis. Cambridge University Press, New York.

644 Olley, J.M., Roberts, R.G., Murray, A.S., 1997. A novel method for determining
645 residence times of river and lake sediments based on disequilibrium in the thorium
646 decay series. *Water Resources Research*, 33(6): 1319-1326.

647 Qin, Y.S., 1994. Sedimentation in northern China seas, *Oceanology of China Seas*.
648 Springer, pp. 395-406.

649 Qin, Y.S., Zhao, Y.Y., Chen, L.R., 1987. *Geology of the East China Sea*. Science
650 Press, Beijing.

651 Russell, A.D., Emerson, S., Nelson, B.K., Erez, J., Lea, D.W., 1994. Uranium in
652 Foraminiferal Calcite as a Recorder of Seawater Uranium Concentrations.
653 *Geochimica Et Cosmochimica Acta*, 58(2): 671-681.

654 Shin, T.-C., Teng, T.-l., 2001. An overview of the 1999 Chi-Chi, Taiwan, earthquake.
655 *Bulletin of the Seismological Society of America*, 91(5): 895-913.

656 Sláma, J., Košler, J., Condon, D.J., Crowley, J.L., Gerdes, A., Hanchar, J.M.,

657 Horstwood, M.S., Morris, G.A., Nasdala, L., Norberg, N., 2008. Plešovice
658 zircon—a new natural reference material for U–Pb and Hf isotopic microanalysis.
659 Chemical Geology, 249(1): 1-35.

660 Suresh, P., Dosseto, A., Handley, H., Hesse, P., 2014. Assessment of a sequential
661 phase extraction procedure for uranium-series isotope analysis of soils and
662 sediments. Applied Radiation and Isotopes, 83: 47-55.

663 Taylor, S.R., McLennan, S.M., 1995. The geochemical evolution of the continental-
664 crust. Reviews of Geophysics, 33(2): 241-265.

665 Ujiié, H., Hiroshi, Tanaka, Y., Ono, T., 1991. Late Quarternary paleoceanographic
666 record from the middle Ryukyu Trench slope, northwest Pacific. Marine
667 Micropaleontology, 18(1–2): 115-128.

668 Ujiié, H., Ujiié, Y., 1999. Late Quaternary course changes of the Kuroshio Current in
669 the Ryukyu Arc region, northwestern Pacific Ocean. Marine Micropaleontology,
670 37(1): 23-40.

671 Vigier, N., Bourdon, B. (Eds.), 2011. Constraining rates of chemical and physical
672 erosion using U-series radionuclides. Handbook of Environmental Isotope
673 Geochemistry, Advances in Isotope Geochemistry. Springer-Verlag, Berlin, 553-
674 571 pp.

675 Wang, J., Li, A., Xu, K., Zheng, X., Huang, J., 2015. Clay mineral and grain size
676 studies of sediment provenances and paleoenvironment evolution in the middle
677 Okinawa Trough since 17ka. Marine Geology, 366: 49-61.

678 White, A.F., Peterson, M.L., 1990. Role of reactive-surface-area characterization in
679 geochemical kinetic models. Chemical Modeling of Aqueous Systems II (eds DC
680 Melchoir and RL Bassett) Chap, 35: 461-475.

681 Yang, S., Bi, L., Li, C., Wang, Z., Dou, Y., 2015. Major sinks of the Changjiang

682 (Yangtze River)-derived sediments in the East China Sea during the late
683 Quaternary. The Geological Society of London, (a special publication on River-
684 Dominated Shelf Sediments of East Asian Seas).

685 Yang, S.Y., Jung, H.S., Li, C.X., 2004. Two unique weathering regimes in the
686 Changjiang and Huanghe drainage basins: geochemical evidence from river
687 sediments. *Sedimentary Geology*, 164(1-2): 19-34.

688 Yu, H., Liu, Z., Berne, S., Jia, G., Xiong, Y., Dickens, G.R., Wei, G., Shi, X., Liu, J.P.,
689 Chen, F., 2009. Variations in temperature and salinity of the surface water above
690 the middle Okinawa Trough during the past 37 kyr. *Palaeogeography*,
691 *Palaeoclimatology, Palaeoecology*, 281(1-2): 154-164.

692

Table 1 Grain size distribution and ($^{234}\text{U}/^{238}\text{U}$) in core DGKS9604 sediments from the Okinawa Trough and in the suspended particles from the Changjiang and Zhuoshui rivers.

Depositional time (ka cal)	Mean grain size ^a (μm)	Sand ^b (%)	Silt ^b (%)	Clay ^b (%)	($^{234}\text{U}/^{238}\text{U}$)
0.1	11.9	3	58	39	1.028 ± 0.001
1.1	11.1	2	59	39	0.988 ± 0.001
1.6	11.1	2	60	38	1.004 ± 0.001
4.1	11.0	2	59	39	1.017 ± 0.002
4.6	10.9	2	60	38	1.040 ± 0.002
7.1	12.2	2	59	39	0.988 ± 0.002
7.6	14.4	3	63	34	0.973 ± 0.002
8.2	12.6	3	59	38	0.979 ± 0.001
8.7	12.6	3	58	39	0.987 ± 0.001
10.2	14.1	4	61	35	1.011 ± 0.000
11.3	13.6	4	58	38	0.962 ± 0.002
11.8	13.0	3	55	42	0.942 ± 0.001
13.0	13.1	4	58	38	0.960 ± 0.002
13.7	12.9	3	64	33	0.942 ± 0.000
13.9	13.5	3	60	37	0.945 ± 0.002
15.8	11.0	1	65	34	0.922 ± 0.003
17.1	10.1	1	62	37	0.940 ± 0.002
18.5	9.7	1	59	40	0.919 ± 0.002
20.2	10.9	2	59	39	0.917 ± 0.002
21.7	11.7	2	61	37	0.923 ± 0.002
22.6	11.5	2	61	37	0.918 ± 0.002
23.3	10.1	1	59	40	0.928 ± 0.001
26.2	12.3	3	57	40	0.922 ± 0.000
27.3	12.8	3	61	36	0.924 ± 0.002
CQ ^c	9.9	0	59	41	0.979 ± 0.002
NT ^c	8.8	0	59	41	0.941 ± 0.001
ZS-1 ^c	11.1	1	74	25	1.002 ± 0.002
ZS-2 ^c	15.4	1	80	19	0.960 ± 0.001

^a Detailed grain size distribution is available in appendix [Table A. 1](#).

^b Relative proportion of sand ($d > 62.5 \mu\text{m}$), silt ($3.9 \mu\text{m} < d < 62.5 \mu\text{m}$), and clay ($< 3.9 \mu\text{m}$).

^c The Changjiang River samples CQ (29.56°N , 106.59°E) and NT (31.96°N , 120.83°E) were collected in the upper and lower reaches, respectively. Samples ZS-1 (23.97°N , 121.11°E) and ZS-2 (23.82°N , 120.21°E) were respectively taken from the upper and lower Zhuoshui River.

Table 2 Recoil loss factors (f_α) and transport times (t_{trans}) calculated with different equations. See the text for the detailed equations and assumptions.

Depositional time (ka cal)	f_α^a $\lambda_{\text{max}}=17$	f_α^a $\lambda_{\text{max}}=2$	T_{trans} $\lambda_{\text{max}}=17$ (kyr)	T_{trans} $\lambda_{\text{max}}=2$ (kyr)	f_α^b $K=18$	f_α^b $K=6$	T_{trans} $K=18$ (kyr)	T_{trans} $K=6$ (kyr)
Core DGKS9604 sediments								
0.1	0.232	0.133	-40	-67	0.280	0.093	-34	-92
1.1	0.233	0.133	18	32	0.280	0.093	14	47
1.6	0.230	0.129	-8	-13	0.272	0.091	-7	-18
4.1	0.233	0.132	-28	-46	0.279	0.093	-24	-62
4.6	0.231	0.130	-61	-100	0.275	0.092	-53	-133
7.1	0.233	0.135	12	26	0.285	0.095	8	41
7.6	0.213	0.119	39	82	0.252	0.084	32	127
8.2	0.229	0.131	26	54	0.277	0.092	20	84
8.7	0.234	0.137	11	26	0.289	0.096	7	42
10.2	0.217	0.121	-28	-41	0.256	0.085	-25	-53
11.3	0.226	0.130	55	113	0.274	0.091	42	181
11.8	0.244	0.149	83	161	0.315	0.105	60	269
13.0	0.228	0.132	55	115	0.279	0.093	42	186
13.7	0.218	0.120	95	216	0.254	0.085	77	388
13.9	0.227	0.131	84	177	0.278	0.093	64	303
15.8	0.224	0.122	136	347	0.258	0.086	112	841
17.1	0.234	0.131	88	200	0.276	0.092	70	357
18.5	0.244	0.141	125	283	0.298	0.099	94	581
20.2	0.237	0.136	132	311	0.287	0.096	100	687
21.7	0.228	0.128	124	303	0.270	0.090	97	656
22.6	0.230	0.129	135	337	0.273	0.091	105	821
23.3	0.239	0.137	103	241	0.288	0.096	78	464
26.2	0.234	0.136	116	274	0.286	0.095	86	568
27.3	0.224	0.126	119	297	0.266	0.089	91	650
River samples								
CQ	0.276	0.177	28	44	0.362	0.121	21	67
NT	0.274	0.170	86	151	0.348	0.116	66	253
ZS-1	0.205	0.105	-3	-6	0.222	0.074	-3	-8
ZS-2	0.183	0.090	86	206	0.191	0.064	82	344

^a f_α calculated from Eq. (2).

^b f_α calculated from Eq. (3).

Figure captions

Figure 1

Map of the East China Sea showing the location of core DGKS9604, the coastline and oceanic circulation at present (a) and during the last glacial maximum (LGM) (b). The LGM coastline is based on the 120 m isobaths (Ujiié and Ujiié, 1999). The major current system in the East China Sea and pathway of the Kuroshio Current is modified from Ichikawa and Beardsley (2002). Transects of the Changjiang catchment to Okinawa Trough (OT) and Taiwan Island to OT are shown in panel (c) and (d), correspondingly. The Changjiang (CQ and NT) and Zhuoshui river (ZS-1 and ZS-2) samples are also indicated in panel (a), (c) and (d).

Figure 2

Downcore profiles [(a) ($^{234}\text{U}/^{238}\text{U}$); (b) CaCO_3 ; (c) Organic carbon (C_{org}); (d) Sulfur in 1N HCl residue; (e) $\text{U}/\text{Al}_2\text{O}_3$; (f) $\text{MnO}/\text{Al}_2\text{O}_3$ and $\text{Fe}_2\text{O}_3/\text{Al}_2\text{O}_3$] in core DGKS9604. Al_2O_3 , Fe_2O_3 and MnO data are from Dou et al. (2012), CaCO_3 from Dou et al. (2010a), total sulfur and organic carbon from Dou (2010).

Figure 3

(a) Changes in mean grain size in Okinawa Trough sediments deposited during the last 27 kyrs, and river particles (e.g. Changjiang (CJ) and Zhuoshui (ZS)). (b) Changes in grain size distribution of the core DGKS9604 sediments and river particles. (c) f_α estimated for marine sediments and river particles. f_α is calculated using Eq. (2) assuming that the surface roughness factor (λ_r) varies from 1 to 2 (DePaolo et al., 2006) and from 1 to 17 (Handley et al., 2013a) with increasing grain size, and using Eq. (3) with a constant surface roughness factor (λ_r) of 7 and grain shape factor (K) varying from 6 to 18 (Cartwright, 1962; Lee et al., 2010).

Figure 4

732 (a) Transport time of the lithogenic fraction in core DGKS9604 sediments. Range of
733 transport times estimated for DGKS9604 are indicated in dark gray (Eq. (2)) and light
734 gray (Eq. (3)). (b) $^{87}\text{Sr}/^{86}\text{Sr}$ ratios in the lithogenic fraction (Dou et al., 2012); (c)
735 Oxygen isotopic ratios in *Globigerinoides sacculifer* (Yu et al., 2009); (d) Sea level
736 variability over the last 30 kyrs (modified after Lambeck et al. (2002)).

Fig. 1

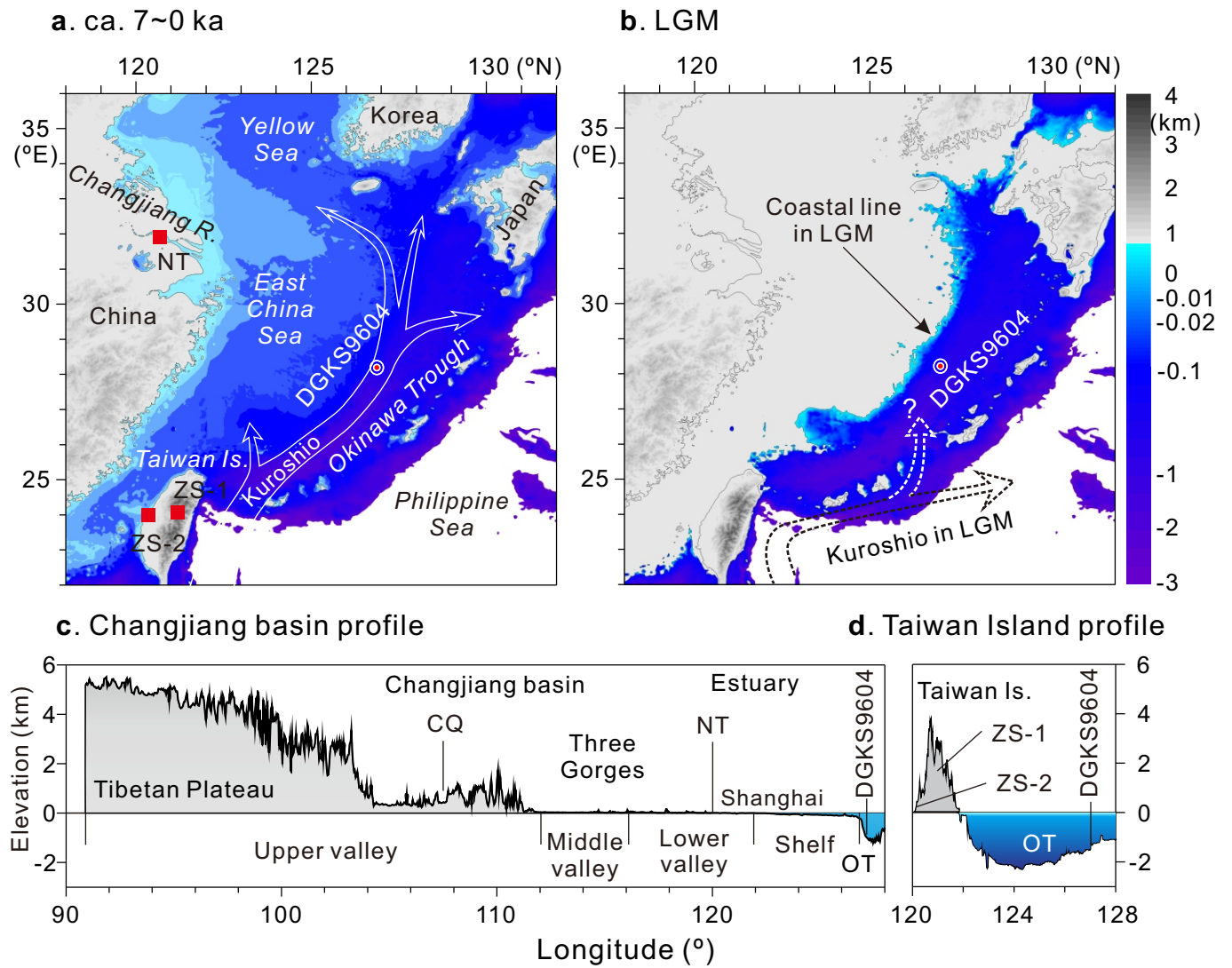


Fig. 2

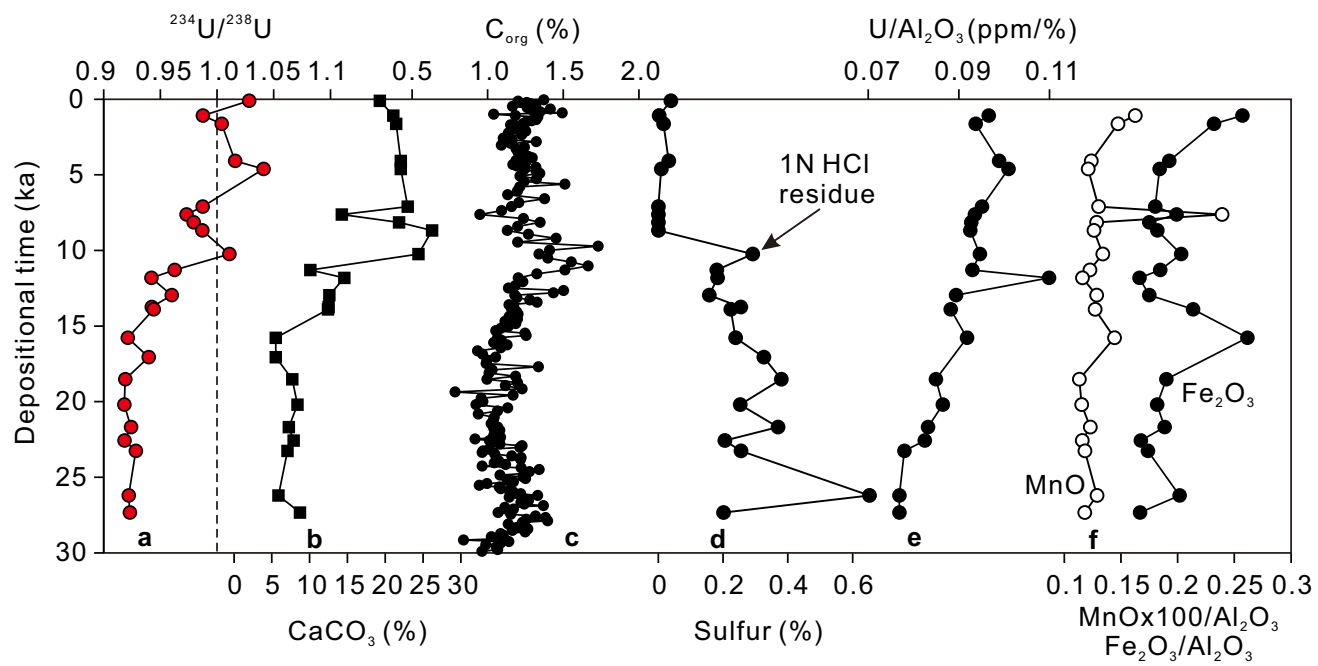


Fig. 3

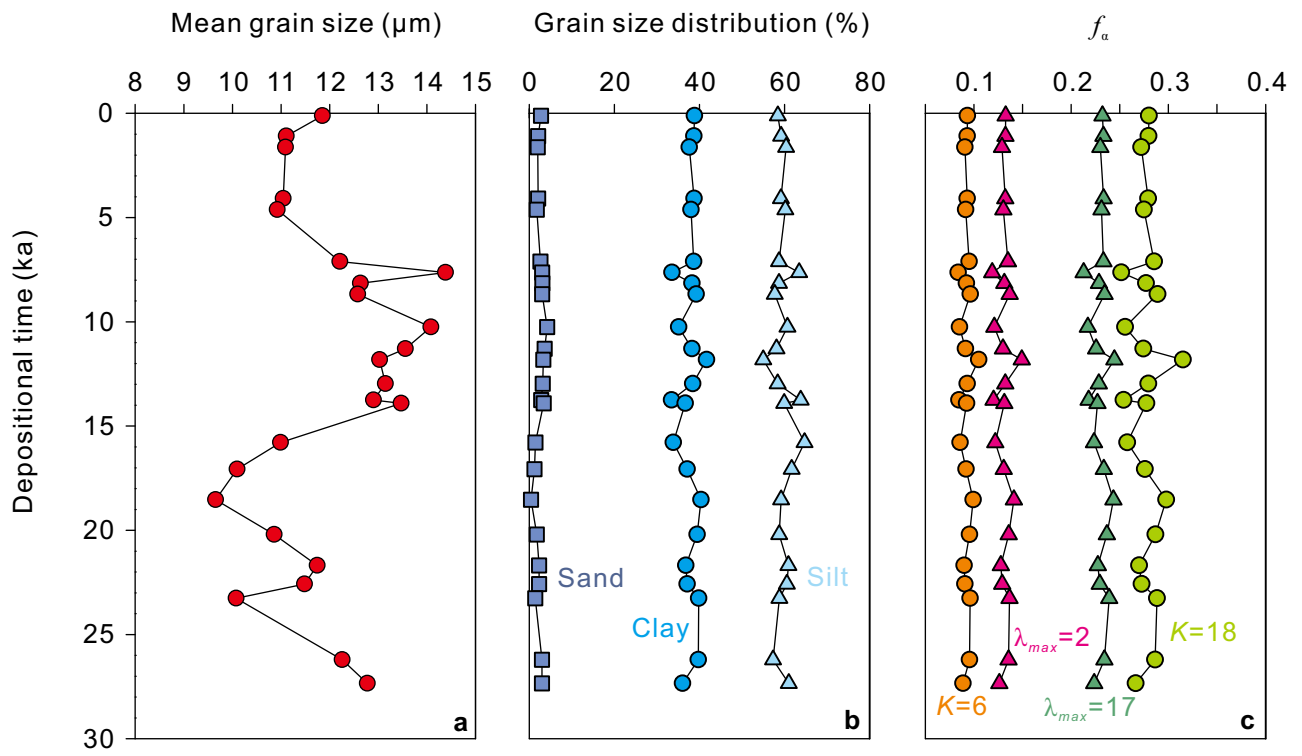
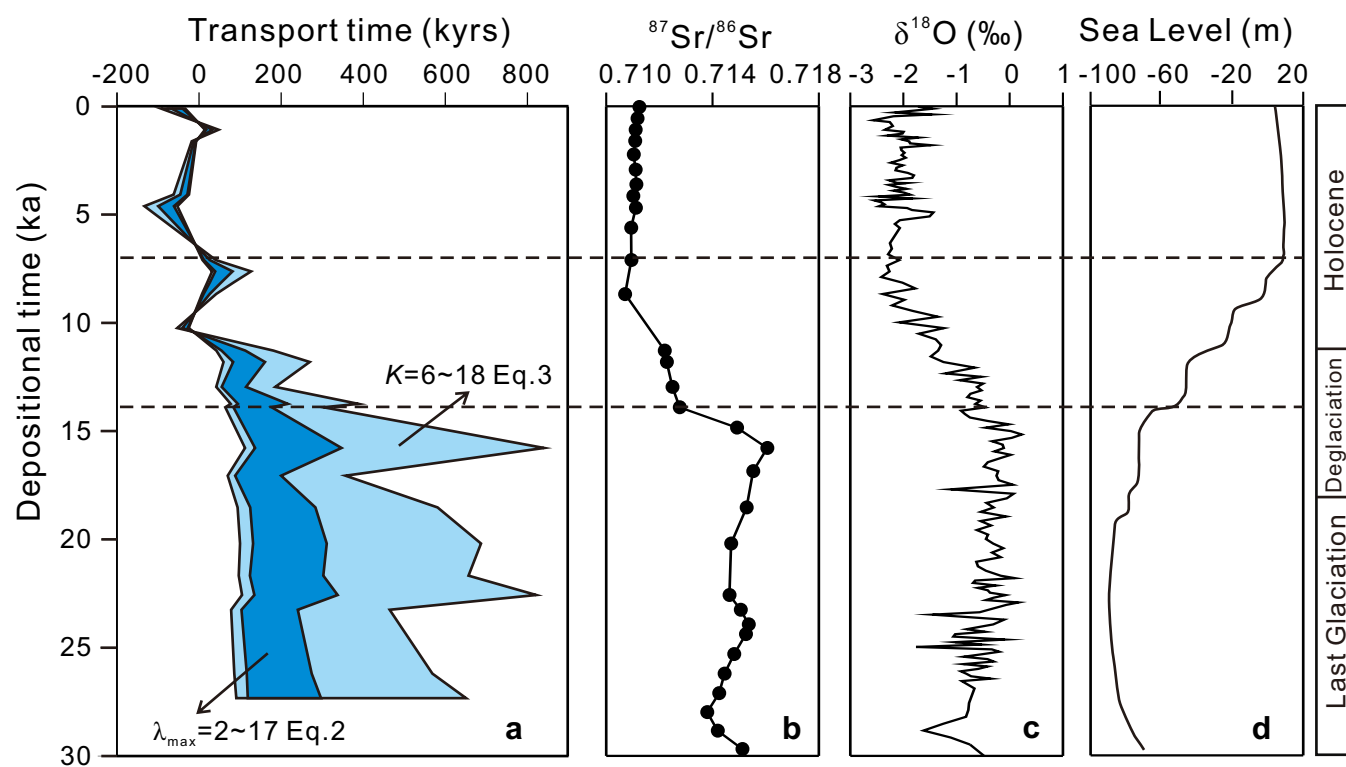


Fig. 4



Appendix tables

[Click here to download Background dataset for online publication only: Appendix Tables.xlsx](#)